

Intersubband spectroscopy by photoconductivity and absorption in inversion layers on p -Si(100)

F. Neppel, J. P. Kotthaus, and J. F. Koch

Physik-Department Technische Universität München, 8046 Garching, Federal Republic of Germany

Y. Shiraki

Hitachi Central Research Laboratory, Tokyo, Japan

(Received 21 March 1977)

Subband spectroscopy in an inversion layer on p -Si(100) is done simultaneously in photoconductivity and absorption. The resonances observed are investigated in their dependence on inversion electron density N_s and depletion charge N_{dep} and are interpreted as transitions from the ground subband to higher subbands of the two valleys with heavy mass perpendicular to the surface. Absorption and photoconductivity give identical resonance positions and similar lineshape. The dependence of the subband splitting on N_s and N_{dep} is found to agree with the measurements of Kneschaurek *et al.* and the most recent theory by Ando. Agreement with the photoconductivity results of Wheeler and Goldberg and the hot-electron-induced emission experiment of Gornik and Tsui can only be achieved if the latter results are assumed to correspond to a much lower N_{dep} than derived from the substrate resistivity at 300 K. In contrast to the results of Wheeler and Goldberg the amplitude of the photoconductivity signal exhibits a strong temperature dependence between 1.7 and 6 K.

I. INTRODUCTION

The investigation of subband energies in n -type inversion layers on Si started with theoretical calculations using the self-consistent Hartree approximation.¹ The experimental determination of the energy separation between the ground and the first excited subband by infrared-absorption measurements^{2,3} was in considerable disagreement with theory. It turned out that the image potential and many-body effects, such as exchange and correlation, needed to be included in a more realistic theory.⁴⁻⁶ Recently, it was pointed out that the measured resonance energies are not the subband energies because of the depolarization effect.^{7,8} The latest calculation of resonance energies by Ando^{9,10} takes into account all these corrections together with the final-state interaction which nearly compensates the depolarization effect. It is in reasonable agreement with the absorption experiment of Kneschaurek *et al.*³

Apart from the infrared-absorption experiment, two other methods have been used to determine subband splittings. Wheeler and Goldberg¹¹ observed resonant photoconductivity caused by excitation of subband transitions. The electron densities N_s at which the resonances occur are about 30% higher than the corresponding N_s values obtained in Ref. 3. No value for the depletion charge N_{dep} is cited in Ref. 11. The doping of the samples gives an equilibrium N_{dep} very similar to the effective N_{dep} in Ref. 3. Furthermore, the photoconductive effect exhibits a line shape completely different from the absorption. Recently, Gornik and Tsui¹² detected hot-electron-induced infrared

emission caused by intersubband transitions. They obtain energy separations in agreement with Ref. 11 that are reported to be independent of the net substrate dopant concentration $N_A - N_D$ between about $1.2 \times 10^{15} \text{ cm}^{-3}$ and $2.2 \times 10^{15} \text{ cm}^{-3}$, corresponding to a N_{dep} varying between 1.3×10^{11} and $1.8 \times 10^{11} \text{ cm}^{-2}$ in thermal equilibrium. This is in disagreement with theory¹⁰ and the substrate bias experiment by Kneschaurek *et al.*¹³ using a substrate bias technique somewhat different from the usual one because of the lack of source-drain contacts.

A comparison of these different results is complicated by the fact that the respective experiments have been carried out on different sets of samples. Kneschaurek *et al.*³ use metal-oxide-semiconductor (MOS) capacitor devices fabricated at the Siemens Forschungslaboratorien, whereas in the work of Refs. 11 and 12 MOS field-effect transistors (MOSFET's) are investigated (produced at Yale University and Bell Laboratories, respectively). The striking discrepancy in resonance energies and line shape and the unexpected lack of influence of $N_A - N_D$ on the subband spectrum¹² raises the question whether the subband energies really depend only on N_s and N_{dep} as predicted by theory. Possibly, the real conditions near the interface, such as inhomogeneity of the doping¹³ or the structure of the Si-SiO₂ transition layer,¹⁴ have a strong effect and need to be included in the theory. Their influence can be of different importance for the various samples because of possible differences in the technological procedures during sample fabrication. In addition, the mechanism causing resonant photoconductivity¹¹ is not yet

well understood and needs further investigation. One theoretical model has been developed by Döhler¹⁵. But so far, the interpretation of the photoconductivity data seems not to be definitive.

The questions mentioned above prompted us to continue the investigation of subband energies by simultaneously measuring absorption and photoconductivity on the same MOSFET. In doing so, we introduce a fourth set of samples into discussion and relate our results to the other experiments and the theory of Ando.¹⁰ After some experimental remarks with emphasis on sample characterization in Sec. II, we discuss in Sec. III A the photoconductive response together with the absorption spectrum and compare our results with those of Ref. 11. In Sec. III B we present the energy separations between the ground state and the first and second excited subband ($E_{0\rightarrow 1}$; $E_{0\rightarrow 2}$) of the two valleys with heavy mass perpendicular to the surface. In a substrate bias experiment, we demonstrate the marked influence of N_{dep} .

II. EXPERIMENTAL REMARKS

The experimental techniques are essentially the same as described in Refs. 3 and 11. The samples are mounted in a transmission-line arrangement.² The MOSFET's used were fabricated by Kotera and Katayama at the Hitachi Central Research Laboratory, Tokyo, on a *p*-type substrate with a room-temperature resistivity $\rho \approx 50 \Omega \text{ cm}$. The area of the Al-gate is $2 \times 2 \text{ mm}^2$, the oxide thickness $d_{\text{ox}} \sim 6500 \text{ \AA}$, the maximum mobility at 4.2 K about $15000 \text{ cm}^2/\text{V sec}$.

Crucial for any comparison of subband energies in different samples is a good knowledge of N_s and N_{dep} . We obtain N_s from Shubnikov-de Haas oscillations (SdH) at 1.7 K. Most of the spectroscopic experiments were carried out at this temperature because of the strong increase of the photoconductive response with decreasing temperature. From SdH we also derive $d_{\text{ox}} = 6370 \text{ \AA}$ in good agreement with capacitance measurements. The inversion threshold is $V_T = 0 \pm 0.1 \text{ V}$, determined by SdH at 1.7 K and the conduction threshold at 77 K. In thermal equilibrium N_{dep} is given by

$$N_{\text{dep}} = [\epsilon_{\text{sl}} E_B (N_A - N_D) / 2\pi e^2]^{1/2}, \quad (1)$$

for a homogeneous net impurity concentration $N_A - N_D$. E_B is the energy difference between the Fermi level and the conduction-band edge in the bulk.⁶ We determine $N_A - N_D$ in several ways: ρ gives $N_A - N_D = 2.6 \times 10^{14} \text{ cm}^{-3}$; *C-V* measurements at 300 K give $N_A - N_D = 2.5 \times 10^{14} \text{ cm}^{-3}$. The third value is derived from the threshold shift ΔV_T induced by a substrate bias voltage V_{SB} . ΔV_T is obtained from the conduction threshold at 77 K and

the SdH threshold at 1.7 K, both methods giving the same result of $N_A - N_D = 2.7 \times 10^{14} \text{ cm}^{-3}$. The latter two methods give $N_A - N_D$ near the inversion layer. In thermal equilibrium and at low temperatures we derive from Eq. (1) $N_{\text{dep}} = 6 \times 10^{10} \text{ cm}^{-2}$.

The presence of band-gap radiation before the measurement favors the equilibrium of the system at low temperatures.¹⁶ The resonance positions remain unchanged within a few percent after the application of light. As a second check for equilibrium we tried to "freeze in" the thermal equilibrium depletion charge by cooling down from 300 to 1.7 K under strong inversion condition. As compared to the case, where no gate voltage was applied during the cooling process, no significant change in resonance positions has been observed. From this and the fact that V_T determined by SdH at 1.7 K coincides with V_T measured as the conduction threshold at 77 K for all substrate bias voltages V_{SB} , we conclude that our experiments are carried out under conditions close to equilibrium. However, repeated thermal cycling between 300 and 1.7 K resulted in some spread of resonance positions to at most $\pm 5\%$. From our substrate bias experiments we interpret this as being caused by a variation in N_{dep} of about $\pm 10\%$. This demonstrates that the thermal equilibrium of the space-charge layer can easily be disturbed. Therefore, N_{dep} derived from $N_A - N_D$ without carefully testing for equilibrium might be in error.

III. RESULTS AND DISCUSSION

A. Photoconduction and absorption signals

Figure 1 shows for a laser energy $\hbar\omega = 10.45 \text{ meV}$ the resonance spectrum for both, photoconductivity and absorption. The total photoconductive response [Fig. 1(a)] consists of a sharp resonance line and a broad background signal of comparable strength, which is independent of laser energy. The response time τ_R of the latter signal contribution is about an order of magnitude larger than the one of the resonant signal. Thus, we are able to separate the resonant response at sufficiently high chopping frequency from the background signal by choosing the appropriate phase in lock-in detection. This is demonstrated in Fig. 1(b). The derivative absorption signal [Fig. 1(c)] shows a resonance at exactly the same position as photoconductivity. The resonance observed in absorption at the lower gate voltage V_g cannot be seen in photoconductivity at this laser energy, since at this energy the resonance occurs at a V_g below the conduction threshold at 1.7 K.

Figure 2 shows the laser-energy dependence of the resonant photoconductivity. At high $\hbar\omega$ the second resonance is also observed. At all laser

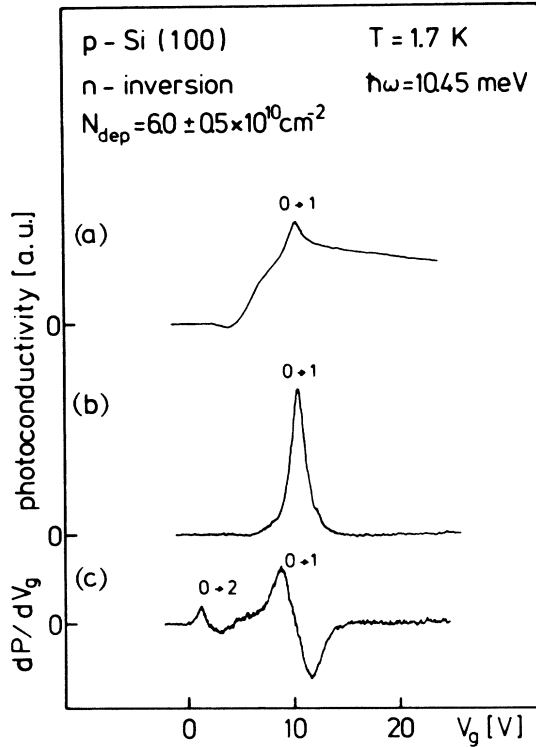


FIG. 1. Total photoconductive response (a), pure resonant photoconductivity at a chopping frequency of 89 Hz (b) and absorption derivative dP/dV_g (c) as a function of gate voltage V_g .

energies the resonance positions in photoconductivity and in the absorption spectrum coincide. We identify the resonances as the 0-1 and 0-2 transitions in the subband system associated with the two valleys with heavy mass perpendicular to the surface. The interpretation of the resonance at lower V_g as the $0' - 1'$ transition in the subband system of the four other valleys has been ruled out because of the behavior of the amplitude ratio of the two resonances under the influence of V_{SB} and temperature.¹⁷

The nonresonant part of the photoconductivity is in a similar way also observable in Siemens and Hitachi MOSFET's with small gate area which do not show the resonant signal. It will be described in detail elsewhere.¹⁸ It is independent of the energy of the exciting radiation between 15.8 meV and microwave energies. For the samples used here, the response time τ_R is found to be roughly 10 msec. The long τ_R , the frequency independence and the signal behavior in a magnetic field¹⁸ suggest that the nonresonant response is caused by heating of the sample. The relevant absorption mechanism is not fully understood, but cannot be direct absorption of the inversion-layer electrons. Therefore, the absorption is independent of V_g and

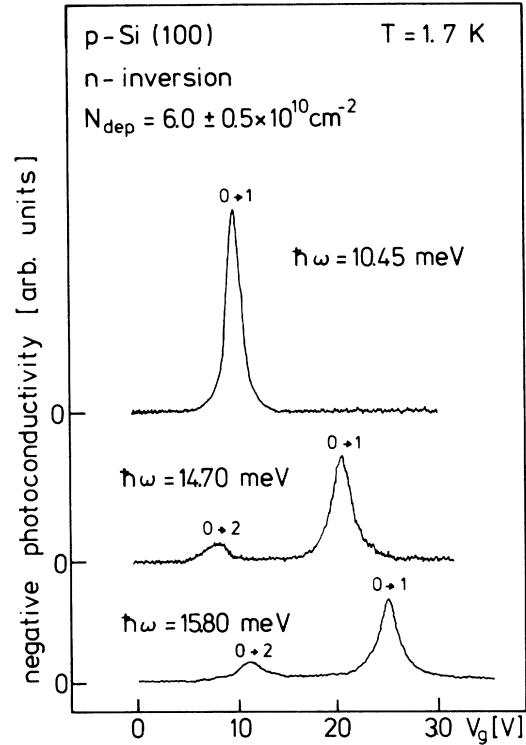


FIG. 2. Resonant photoconductive response as a function of gate voltage V_g at different laser energies $\hbar\omega$.

cannot be seen in the absorption derivative with respect to V_g . The observed V_g dependence of this part of the photoconductivity, being positive for small N_s and negative for higher N_s , simply reflects the temperature dependence of the mobility in the inversion channel.

The resonant part of the photoconductivity usually consists of two distinct narrow lines, which agree in position, line shape, and linewidth with the corresponding resonances found in absorption. Because the resonances are very narrow, the correction with respect to the field-effect mobility μ_{FE} ¹¹ has no noticeable effect on the line shape of a single photoconductive resonance. It is only important for a comparison of the amplitudes of the two resonances. In photoconductivity the amplitude ratio $A_{0 \rightarrow 1}/A_{0 \rightarrow 2}$, corrected for μ_{FE} , tends to be a factor of two larger than in absorption, indicating a larger mobility change for the 0-1 resonance. Possibly this might show, however, that the μ_{FE} scaling is not justified at all. At resonance, the relative conductivity change is typically 10^{-4} for the 0-1 transition and negative for all values of $\hbar\omega$. The response time τ_R is of order 1 msec. The linewidths correspond to lifetimes τ of about 10^{-12} sec. With $\hbar\omega = 15.8 \text{ meV}$, we obtain for the 0-1 resonance $\tau = 1.7 \times 10^{-12}$ sec, com-

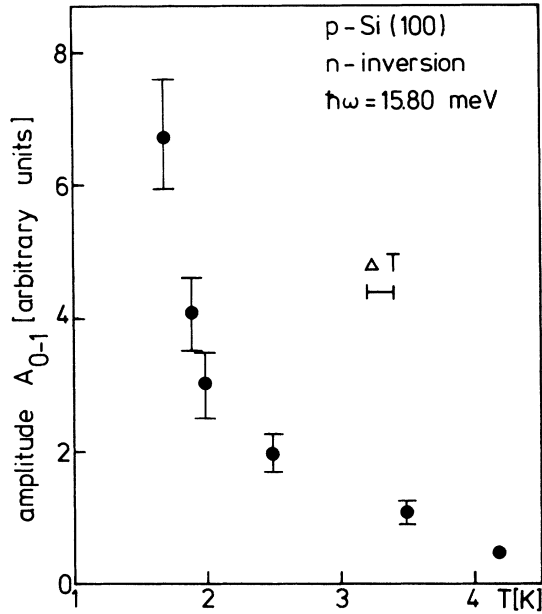


FIG. 3. Temperature dependence of the amplitude A_{0-1} of the photoconductive $0 \rightarrow 1$ resonance at $\hbar\omega = 15.80$ meV.

pared to $\tau = 1.6 \times 10^{-12}$ sec derived from mobility at 1.7 K.

The amplitude of the resonant photoconductivity is strongly temperature dependent (Fig. 3). Cooling down from 4.2 to 1.7 K results in an enhancement of the signal by a factor of 15. Above 6 K, the resonant photoconductivity can no longer be observed. For the small temperature range, the data are not accurate enough to extract the exact functional dependence. The absorption, the resonance positions, and the line shape do not change noticeably between 1.7 and 6 K.

There are two significant differences in the photoconductive response described here and in Ref. 11: the line shape and the temperature dependence. We observe two narrow resonances, Wheeler and Goldberg one narrow resonance together with a broad, but likewise $\hbar\omega$ -dependent precursor at lower V_g . The strong temperature dependence at liquid-helium temperatures mentioned above is in contrast to the temperature independence in this range found in Ref. 11. The difference between lifetime τ and response time τ_R by about nine orders of magnitude seems to be a general feature of the resonant photoconductivity. It is not explained by the simple model assumed in Ref. 11 that takes into account only the two directly interacting subbands. In a one-particle model, at least one intermediate level needs to be introduced. Döhler suggested the ground subband of the four valleys with light mass perpendicular to the surface to be this level.¹⁵ His model, how-

ever, does not account for the observed size and temperature dependence of the photoconductivity.

Possibly the one-particle model is not applicable at all, and many-body interaction has to be considered to explain photoconductivity. The absorption of infrared radiation causes a redistribution of charge near the interface, which might change the scattering rate for all electrons.

B. Resonance energies

Figure 4 shows the energy difference E_{0-1} between the ground and the first excited subband as a function of N_s for our samples ($N_{dep} = 6 \times 10^{10}$ cm⁻²) together with the results of Refs. 3, 10-12. Unfortunately, the doping and hence N_{dep} according to Eq. (1) is not the same for all experiments. We have no calculation for $N_{dep} = 6 \times 10^{10}$ cm⁻², but our results are qualitatively consistent with theory¹⁰ and also with the experiment of Kneschaurek *et al.*,³ which is carried out on samples different from ours. With increasing N_{dep} , one expects the subband splitting to increase, i.e., at constant $\hbar\omega$, the resonance to occur at lower N_s . In that respect there is disagreement with the results of Refs. 11 and 12, if one assumes a N_{dep}

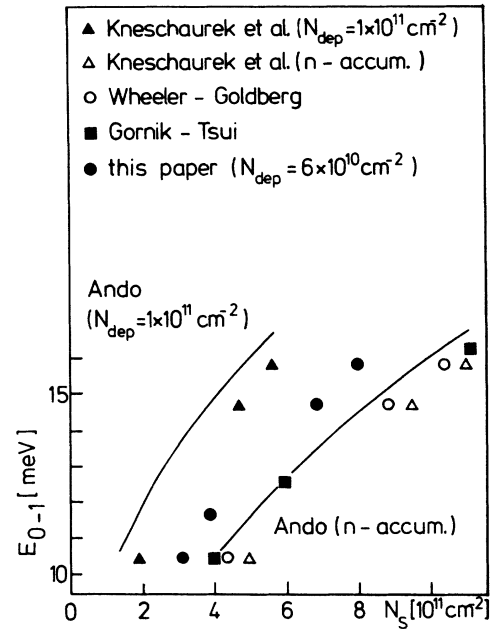


FIG. 4. Energy separations E_{0-1} between ground subband and the first excited subband as a function of electron density N_s for different sets of samples (Refs. 3, 11, 12, and this paper). The depletion charge N_{dep} for the experiments of Wheeler-Goldberg and Gornik-Tsui, derived from room-temperature resistivity ρ using Eq. (1) is 1×10^{11} cm⁻² and 1.2×10^{11} cm⁻², respectively. The curves are taken from Ando's work (Ref. 10).

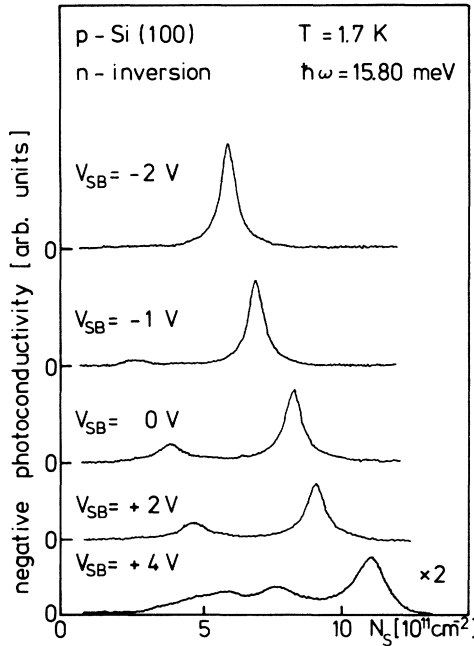


FIG. 5. Resonant photoconductive response to 15.8 meV radiation as a function of electron density N_s at various values of V_{SB} .

derived from Eq. (1) and the given dopant concentrations.

For a quantitative comparison with theory and the other experiments, we made use of substrate bias to vary N_{dep} . In doing so, the strong influence of N_{dep} on resonance positions becomes evident. Figure 5 shows the photoconductive spectrum for several values of V_{SB} . For a negative V_{SB} and in thermal equilibrium, N_{dep} is given by Eq. (1), with E_B/e replaced by $E_B/e + V_{SB}$. Thus, a negative V_{SB} increases N_{dep} . For high positive values of V_{SB} no analytical expression is available, but a decrease of N_{dep} is expected. Positive V_{SB} and band-gap radiation have the same effect on V_T and the resonances, and band-gap radiation is known to decrease N_{dep} .³ The shift of the 0-1 resonances to higher N_s with increasing positive V_{SB} tends to saturate. For $V_{SB} \geq +4$ V resonance positions and line shapes do not change significantly. Under this strong forward-bias condition new lines, interpreted as higher-order transitions (0-3, ...), appear at lower V_g and pile up with the 0-2 resonance somewhat below the 0-1 resonance (lowest trace in Fig. 5). In this case, the line shape becomes quite similar to the one calculated for n^- accumulation,¹⁰ which has been verified experimentally by Kneschaurek *et al.*³ We interpret the strong forward bias condition as a quasiaccumulation situation.

In Fig. 6, E_{0-1} is plotted as a function of N_s for

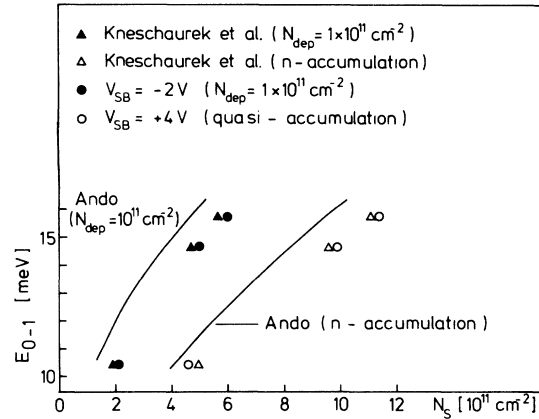


FIG. 6. Energy separation E_{0-1} as a function of electron density N_s for different values of the depletion charge N_{dep} . Also plotted are the experimental values of Kneschaurek *et al.* (Ref. 3) and the calculations of Ando (Ref. 10).

two different values of V_{SB} . $V_{SB} = -2$ V corresponds to $N_{dep} = 1 \times 10^{11} \text{ cm}^{-2}$, the N_{dep} of the samples used in Ref. 3. For this N_{dep} as well as for the quasiaccumulation, the good agreement with the results of Kneschaurek *et al.*³ and the calculated subband splittings¹⁰ is obvious. We note that E_{0-1} for quasiaccumulation is close to the subband splitting measured in Refs. 11 and 12. The substrate bias experiments give an average change of E_{0-1} with N_{dep} of $4.5 \text{ meV}/10^{11} \text{ cm}^{-2}$ for $1 \times 10^{11} \text{ cm}^{-2} \leq N_s \leq 8 \times 10^{11} \text{ cm}^{-2}$. Ando gives $4.1 \text{ meV}/10^{11} \text{ cm}^{-2}$ for $1 \times 10^{11} \text{ cm}^{-2} \leq N_s \leq 2.25 \times 10^{11} \text{ cm}^{-2}$, Kneschaurek $3.4 \text{ meV}/10^{11} \text{ cm}^{-2}$ for $0.45 \times 10^{11} \text{ cm}^{-2} \leq N_s \leq 6 \times 10^{11} \text{ cm}^{-2}$.

As expected, the substrate bias effect on the 0-2 resonance is more pronounced. The wave functions in the higher subbands extend much more into the depletion layer. Therefore, these states are more sensitive to changes in N_{dep} and the corresponding potential. Figure 7 shows E_{0-2} as a function of N_s for $N_{dep} = 6 \times 10^{10} \text{ cm}^{-2}$ and quasiaccumulation. The lack of calculations for $N_{dep} = 6 \times 10^{10} \text{ cm}^{-2}$ only allows us to compare the quasiaccumulation data with theory.¹⁰ The discrepancy between theory and experiment might be caused by the fact that, as pointed out by Ando,¹⁰ the calculation does not take into account sufficiently the mixing between the various subbands at small-subband splittings. Corresponding corrections would bring theory closer to the experimental values. Since this effect is strongest at low N_s , one expects the difference between theory and experiment to decrease with increasing N_s , as is observed. The energy separation for the 0-2 transition is 10.45 meV at $N_s = 0$ and $N_{dep} \approx 8 \times 10^{10} \text{ cm}^{-2}$. This is obtained from an absorption experi-

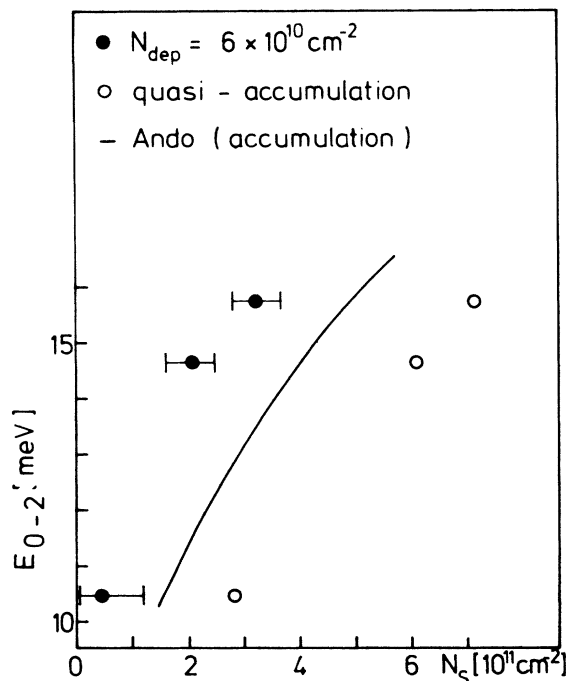


FIG. 7. Energy separation E_{0-2} between the ground subband and the second excited subband vs electron density N_s for a depletion charge $N_{\text{dep}} = 6 \times 10^{10} \text{ cm}^{-2}$ and quasiaccumulation. Ando's calculation for n -accumulation is also shown.

ment with substrate bias at the corresponding laser energy.

IV. CONCLUDING REMARKS

We have shown that photoconductivity and absorption measurements give identical resonances. Using Hitachi MOSFET's we have confirmed the

subband energies obtained by Kneschaurek *et al.*³ on Siemens MOS-capacitor devices and have demonstrated the importance of N_{dep} . To properly characterize spectroscopy data, N_{dep} must be determined. To do this just from ρ , however, is not reliable and might be in error for the following reasons. The dopant concentration may be inhomogeneous. Further, the inversion channel and the substrate are possibly not in thermal equilibrium at low temperatures because they are separated by the insulating depletion layer. Simple checks for both cases are outlined in the experimental section. Only the knowledge of the correct N_{dep} in the various subband spectroscopy experiments will allow us to investigate, e.g., the influence of the real structure of the Si-SiO₂ transition layer.

One possibility to account for the discrepancies between the results of Wheeler and Goldberg,¹¹ Gornik and Tsui,¹² and our data is to assume the experiments of Refs. 11 and 12 as having been carried out under quasiaccumulation conditions for either one of the two reasons mentioned above. The resonance positions and line shape (not available in Ref. 12) described there are similar to the data we obtain for the quasiaccumulation condition (see last trace in Fig. 5 and the plots of $E_{0 \rightarrow 1}$ vs N_s in Figs. 4 and 6). Our forward-bias experiment suggests that the broad precursor peak observed by Wheeler and Goldberg contains contributions of unresolved higher-order transitions.

ACKNOWLEDGMENTS

We wish to thank Dr. Kotera and Dr. Katayama for fabricating the samples and Professor Wheeler for valuable discussions. The financial support by Deutsche Forschungsgemeinschaft via Sonderforschungsbereich SFB 128 is gratefully acknowledged.

¹F. Stern, Phys. Rev. B **5**, 4891 (1972).

²A. Kamgar, P. Kneschaurek, G. Dorda, and J. F. Koch, Phys. Rev. Lett. **32**, 1251 (1974).

³P. Kneschaurek, A. Kamgar, and J. F. Koch, Phys. Rev. B **14**, 1610 (1976).

⁴F. Stern, Phys. Rev. Lett. **30**, 278 (1973).

⁵B. Vinter, Phys. Rev. B **13**, 4447 (1976); **15**, 3947 (1977).

⁶T. Ando, Phys. Rev. B **13**, 3468 (1976).

⁷W. B. Chen, Y. J. Chen, and E. Burstein, Surf. Sci. **58**, 263 (1976).

⁸S. J. Allen, D. C. Tsui, and B. Vinter, Solid State Commun. **20**, 425 (1976).

⁹T. Ando, Solid State Commun. **21**, 133 (1976).

¹⁰T. Ando, Z. Phys. **26**, 263 (1977).

¹¹R. G. Wheeler and H. S. Goldberg, IEEE Trans. Electron. Devices ED-22, 1001 (1976).

¹²E. Gornik and D. C. Tsui, Phys. Rev. Lett. **37**, 1425 (1976).

¹³A. S. Grove, O. Leistiko, and C. T. Sah, J. Appl. Phys. **35**, 2695 (1964).

¹⁴F. Stern, Solid State Commun. **21**, 163 (1977).

¹⁵G. H. Döhler, Solid State Commun. **18**, 633 (1976).

¹⁶A. B. Fowler, Phys. Rev. Lett. **34**, 15 (1975).

¹⁷P. Kneschaurek and J. F. Koch, Phys. Rev. B (to be published).

¹⁸Y. Shiraki (unpublished).

¹⁹R. G. Wheeler, C. C. Hu, and K. Cham (unpublished).